




Absence of canonical trophic levels in a microbial mat

Ana C. Gonzalez-Nayeck¹  | Wiebke Mohr^{1,2}  | Tiantian Tang^{1,3,4} | Sarah Sattin¹ |
M. Niki Parenteau⁵ | Linda L. Jahnke⁵  | Ann Pearson¹

¹Department of Earth and Planetary Sciences, Harvard University, Cambridge, Massachusetts, USA

²Max-Planck-Institute for Marine Microbiology, Bremen, Germany

³State Key Laboratory of Marine Environmental Science (Xiamen University), Xiamen, Fujian, China

⁴College of Ocean and Earth Sciences, Xiamen University, Xiamen, Fujian, China

⁵NASA Ames Research Center, Moffett Field, California, USA

Correspondence

Ana C. Gonzalez-Nayeck, Department of Earth and Planetary Sciences, Harvard University, Cambridge, MA, USA.
Email: gonzalezvaldes@g.harvard.edu

Funding information

Gordon and Betty Moore Foundation; Marie Curie; National Science Foundation

Abstract

In modern ecosystems, the carbon stable isotope ($\delta^{13}\text{C}$) ratios of consumers generally conform to the principle “you are what you eat, +1‰.” However, this metric may not apply to microbial mat systems where diverse communities, using a variety of carbon substrates via multiple assimilation pathways, live in close physical association and phagocytosis is minimal or absent. To interpret the $\delta^{13}\text{C}$ record of the Proterozoic and early Paleozoic, when mat-based productivity likely was widespread, it is necessary to understand how a microbially driven producer–consumer structure affects the $\delta^{13}\text{C}$ compositions of biomass and preservable lipids. Protein Stable Isotope Fingerprinting (P-SIF) is a recently developed method that allows measurement of the $\delta^{13}\text{C}$ values of whole proteins, separated from environmental samples and identified taxonomically via proteomics. Here, we use P-SIF to determine the trophic relationships in a microbial mat sample from Chocolate Pots Hot Springs, Yellowstone National Park (YNP), USA. In this mat, proteins from heterotrophic bacteria are indistinguishable from cyanobacterial proteins, indicating that “you are what you eat, +1‰” is not applicable. To explain this finding, we hypothesize that sugar production and consumption dominate the net ecosystem metabolism, yielding a community in which producers and consumers share primary photosynthate as a common resource. This idea was validated by confirming that glucose moieties in exopolysaccharide were equal in $\delta^{13}\text{C}$ composition to both cyanobacterial and heterotrophic proteins, and by confirming that highly ^{13}C -depleted fatty acids (FAs) of Cyanobacteria dominate the lipid pool, consistent with flux-balance expectations for systems that overproduce primary photosynthate. Overall, the results confirm that the $\delta^{13}\text{C}$ composition of microbial biomass and lipids is tied to specific metabolites, rather than to autotrophy versus heterotrophy or to individual trophic levels. Therefore, we suggest that aerobic microbial heterotrophy is simply a case of “you are what you eat.”

1 | INTRODUCTION

Modern analogs are essential when contextualizing the carbon ($\delta^{13}\text{C}$) isotope ratios of organic matter from ancient ecosystems. Modern microbial mats may help illuminate Precambrian environments, given the prevalence of stromatolites in Archean rocks (Awramik, 1992; Hoffman, 2000; Schopf et al., 2007; Djokic et al., 2021), the observation of microbial textures in Proterozoic rocks (Callow &

Brasier, 2009; Gehling, 1999; Hagadorn & Bottjer, 1997; Steiner & Reiter, 2001), and evidence that bioturbation did not reach modern intensity until the mid-Paleozoic (Tarhan, 2018). Furthermore, non-lithifying (i.e., non-stromatolite) microbial mats, which represent the majority of modern mat morphologies but are poorly preserved in the geologic record, might represent the majority of mat-based carbon fixation during the Precambrian (Schuler et al., 2017). Despite this importance, microbial mats – with complex diversity yet few

taxa capable of phagocytosis – are not easily classified by canonical ecosystem methods (Anderson et al., 1987; van der Meer et al., 2007; Flemming & Wingender, 2010; Klatt et al., 2013; Stuart et al., 2016; Hamilton et al., 2019; Bennett et al., 2020). There are numerous indications that the macrofaunal concept of “trophic levels” should be avoided in mat-dominated ecosystems. Some consumer taxa in mats are strictly heterotrophic, while others are mixotrophic or have flexible carbon metabolisms (Bennett et al., 2020; Hamilton et al., 2019; Klatt et al., 2013; van der Meer et al., 2007). One of the major organic carbon sources in mats, the binding matrix of extracellular polymeric substances (EPS, mostly exopolysaccharide), can be accessed by heterotrophic organisms via either extracellular digestion to monomers or by fermentation to smaller carbon units before assimilation (Anderson et al., 1987; Flemming & Wingender, 2010; Stuart et al., 2016). This complexity introduces challenges for reconstructing the flow of carbon and energy resources in past environments using the classical methods of geobiology and isotope geochemistry.

Trophic levels and the structure of modern, macrofaunal ecosystems traditionally are investigated through the lens of carbon ($\delta^{13}\text{C}$) and nitrogen ($\delta^{15}\text{N}$) isotope ratios (Cabana & Rasmussen, 1996; Fry & Sherr, 1984). The colloquial phrase “you are what you eat, +1‰,” is grounded in a study of the $\delta^{13}\text{C}$ values of small animals capable of holozoic feeding when grown on a complex diet, while simultaneously disguising the underpinning molecular-level heterogeneity that comprises both the food and the consumer (DeNiro & Epstein, 1978). For example, $\delta^{13}\text{C}$ values for individual biochemical fractions from a fly fed horsemeat ranged from approximately 3‰ more negative (lipids) to 1‰ more positive (soluble protein) than the horsemeat substrate. This distribution is expected, given the fractionation associated with lipid synthesis (DeNiro & Epstein, 1977; Melzer & Schmidt, 1987; Monson & Hayes, 1982). It also reinforces that “you are what you eat, + 1‰” may only apply to organisms that consume whole prey, ingest herbaceous material, filter-feed on a diet of zooplankton, or can engulf whole microbes (Fry & Sherr, 1984; Fantle et al., 1999; Pinnegar & Polunin, 2000; van der Zanden & Rasmussen, 2001). By contrast, microbes incapable of phagocytosis selectively utilize specific substrates (Arnosti et al., 2011; Mahmoudi et al., 2017). Concomitantly, most bacteria repress the expression of catabolic enzymes for secondary carbon sources in the presence of their preferred substrate (Görke & Stülke, 2008).

Despite these arguments that microbial ecosystems should not have trophic organization, the “you are what you eat, +1‰” concept is used in the geobiological and geochemical literature as an estimate for the $\delta^{13}\text{C}$ signature of microbial heterotrophy, typically in the context of using lipid biomarkers to probe the ecology of ancient systems (e.g., Close et al., 2011; Logan et al., 1995; Luo et al., 2015; Pawlowska et al., 2013; van Maldegem et al., 2019). The rationale stems from generalizing the idea of an expressed fractionation during respiratory decarboxylation (Blair et al., 1985), resulting in the assumption that all heterotrophs would be systematically enriched in ^{13}C relative to autotrophs. However, as previously noted by Breteler et al. (2002), even the data from DeNiro and Epstein (1978)

show a range in respired carbon $\delta^{13}\text{C}$ values from +1.4‰ to –3.5‰ relative to the food, which is expected as this value will vary depending on the proportion of CO_2 derived from the decarboxylation of pyruvate (relatively ^{13}C -enriched) versus the decarboxylation of Krebs Cycle intermediates (relatively ^{13}C -depleted) (Hayes, 2001). Nonetheless, the assumption of a 1‰ enrichment in heterotrophic biomass has been used to interpret the $\delta^{13}\text{C}$ patterns observed in both modern (e.g., Musilova et al., 2015; Pedrosa-Pàmies et al., 2018) and ancient (e.g., Osterhout et al., 2021; Williford et al., 2013) bulk organic matter, and in various biochemical fractions relative to one another (e.g., Close et al., 2011; Logan et al., 1995; Luo et al., 2015; Pawlowska et al., 2013; van Maldegem et al., 2019). Alternative hypotheses for the ^{13}C enrichments observed in microbial systems include diagenetic overprinting (Vinnichenko et al., 2021), a relatively greater assimilation of ^{13}C -enriched substrates like acetate (Blair et al., 1985; Penning & Conrad, 2006), or increased fractional contributions from alternative metabolisms (House et al., 2003; van der Meer et al., 2001). It therefore remains critical to understand how, or if, a $\delta^{13}\text{C}$ signature of microbial heterotrophy would be preserved in the rock record.

To date, a major obstacle in this effort has been measuring taxonomically resolved, natural abundance $\delta^{13}\text{C}$ values for microbial communities at sub-1‰ resolution. Prior studies comparing the $\delta^{13}\text{C}$ values of phylum-specific biomarker lipids consistently report measurements at sub-1‰ resolution (e.g., Jahnke et al., 2004; Jahnke & des Marais, 2019; van der Meer et al., 2003; Werne et al., 2002). However, using these data to estimate the $\delta^{13}\text{C}$ values of autotrophic and heterotrophic microbial biomass is infeasible, given the variable offset in $\delta^{13}\text{C}$ values between lipids and biomass (Blair et al., 1985; DeNiro & Epstein, 1977; Tang et al., 2017). Protein Stable Isotope Fingerprinting (P-SIF) is a novel method for measuring the $\delta^{13}\text{C}$ values of whole proteins that have been separated from environmental samples and classified taxonomically via proteomics (Mohr et al., 2014). Because $\delta^{13}\text{C}$ values of proteins scale directly with biomass $\delta^{13}\text{C}$ values (Abelson & Hoering, 1961; Blair et al., 1985), this approach yields taxon-specific or group-specific $\delta^{13}\text{C}$ signatures of organisms. Although P-SIF has only modest taxonomic resolving power, it has several advantages that complement other recent stable isotope approaches (e.g., Dekas et al., 2019; Kleiner et al., 2018; Mayali et al., 2012; Radajewski et al., 2000): it does not require addition of isotope labels, incubations, or novel calibrations, and it has a mean analytical precision <1‰.

Here, we use P-SIF to assign $\delta^{13}\text{C}$ values for taxonomic groups in a previously characterized Cyanobacteria–Chloroflexi mat from Chocolate Pots Hot Springs (CP; Figure 1), Yellowstone National Park, USA (Klatt et al., 2013; Pierson et al., 1999; Pierson & Parenteau, 2000). We also report fatty acid (FA) $\delta^{13}\text{C}$ values to relate the protein data to lipid biomarkers that can be preserved over geologic time scales. Our results show that the canonically heterotrophic groups of organisms in the Chocolate Pots (CP) mat are isotopically indistinguishable from both the photoautotrophic Cyanobacteria and the sugar moieties of extracellular polymeric substances (EPS) produced by those Cyanobacteria. By contrast, the filamentous anoxygenic phototrophic

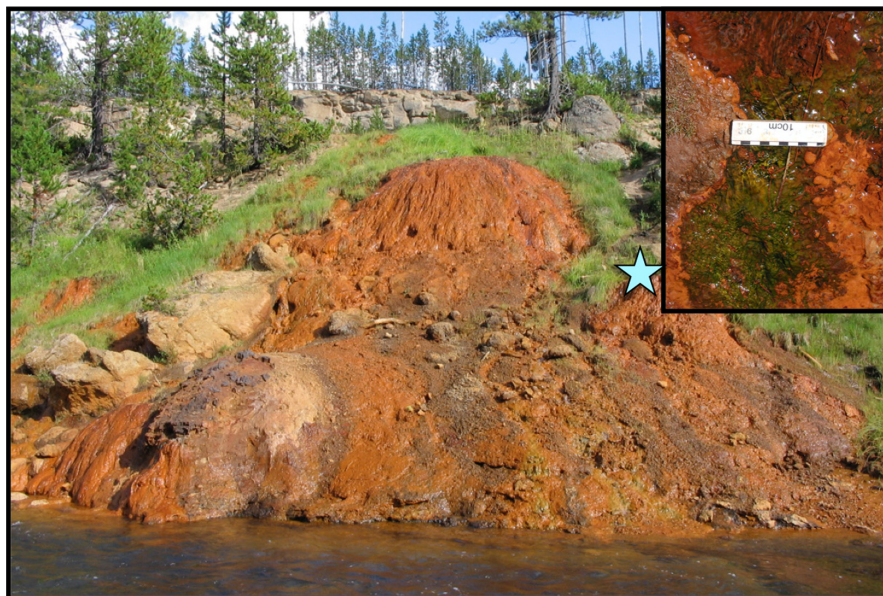


FIGURE 1 Chocolate Pots Hot Springs in Yellowstone National Park (YNP). Blue star indicates sampling location for this study. Photograph on the upper right is a close-up of the *Synechococcus*-*Chloroflexi* mat. Photographs by N. Parenteau

(FAP) *Chloroflexi* are moderately enriched in ^{13}C due to their mixotrophic lifestyle. These results indicate that high-density microbial communities do not conform to “you are what you eat +1‰”, which we hypothesize is likely due to EPS-driven feeding and the complexities of small-molecule resource sharing.

2 | MATERIALS AND METHODS

2.1 | Sample collection

Chocolate Pots Hot Springs (CP) contains four types of phototrophic microbial mats: *Synechococcus*-*Chloroflexi* (50–54°C), *Pseudanabaena* spp. (50–54°C), narrow *Oscillatoria* spp. (36–45°C), and *Oscillatoria* cf. *princeps* (37–47°C) (Pierson et al., 1999; Pierson & Parenteau, 2000). *Synechococcus*-*Chloroflexi* mat samples, the focus of this study, were collected in August 2014 under Yellowstone National Park Research Permit number 1549 and immediately placed on dry ice at the field site. A sample of approximately 15 grams was shipped to the laboratory on dry ice and subsequently frozen at -80°C until analysis. The sample was taken from the same location sampled for the YNP Metagenome Project (Inskeep et al., 2013; Klatt et al., 2013).

At collection, the pH of the vent water flowing over the mat was 6.1 and the temperature was 49.7°C . No further geochemical parameters were measured at the time of sampling; however, prior work on vent waters at Chocolate Pots Hot Springs (CP) has shown that the concentrations of various species have changed little over 80 years (see Table 2 from Parenteau & Cady 2010).

2.2 | Lipid extraction and identification

Lipids were extracted from approximately 0.3 g (dry) of freeze-dried mat samples via a modified Bligh and Dyer procedure (Sturt

et al., 2004). The total lipid extract was transesterified to generate fatty acid methyl esters (FAMES; 5% HCl/methanol [v/v], 70°C , 4 h). The reaction was stopped by the addition of ultrapure H_2O , after which the organic phase was extracted into hexane/dichloromethane (4:1, v/v). FAME derivatives of *n*- $\text{C}_{16:0}$, *n*- $\text{C}_{19:0}$, and *n*- $\text{C}_{24:0}$ FA standards with known $\delta^{13}\text{C}$ compositions (-29.5% , -31.7% , and -30.8% , respectively) were prepared in parallel to correct for the ^{13}C content of the derivatized carbon introduced during transesterification. FAMES were further separated from the derivatized extract by elution over SiO_2 gel using the solvent program described in (Pearson et al., 2001).

The FAMES were identified using gas chromatography-mass spectrometry (GC/MS; Agilent 6890N GC, 5973 MS equipped with a 30m DB-5MS column) by comparison to known patterns of relative retention times (Pearson et al., 2001; Perry et al., 1979) and by comparison of fragment mass spectra to spectra from the National Institute of Standards and Technology Library (Shen et al., 2017). The injection, oven temperature programs, and gas flow rates were adopted from Close et al., 2014.

2.3 | Protein stable isotope fingerprinting

Protein Stable Isotope Fingerprinting (P-SIF) was performed as previously described (Mohr et al., 2014). Proteins were extracted from microbial mat samples by placing approximately 7 grams of wet mat material and up to 8 ml of bacterial protein extraction reagent (B-PER) protein extraction reagent (Thermo Scientific) in a 50 ml Teflon tube and sonicating using a 500-watt Qsonica ultrasonic processor equipped with a cup horn. The cup horn was filled with ice water and the sonicator was set to 25 s on and 35 s off for a total of 5 min sonication. Solids and cell material were removed by centrifugation at 16,000g. Proteins were precipitated from the supernatant in acetone and resuspended in 100 mM

NH_4HCO_3 , pH 9 to yield a total soluble protein extract. This extract was further separated into 960 fractions on an Agilent 1100 series HPLC with diode-array detector (DAD) and fraction collector using two orthogonal levels of chromatography: first by strong anion exchange (SAX; Agilent PL-SAX column; 4.6×50 mm, $8 \mu\text{m}$) (20 fractions), then by reverse phase (RP; Agilent Poroshell 300SB-C3 column, 2.1×75 mm, $5 \mu\text{m}$; 48 fractions), using the solvent gradients described in (Mohr et al., 2014). An aliquot of each final fraction is split into 96-well plates for isotope analysis (70%) and the remaining 30% is reserved for tryptic digestion followed by peptide sequencing.

2.4 | Protein taxonomic identification

Plates for tryptic digestion were prepared as detailed in (Mohr et al., 2014). Peptides were sequenced by capillary liquid chromatography–tandem mass spectrometry (LC–MS/MS) using an Agilent 1200 Series HPLC equipped with a Kinetex C_{18} column ($2.1 \text{ mm} \times 100 \text{ mm}$, $2.6 \mu\text{m}$ particles) and an Agilent 6520 quadrupole time-of-flight mass spectrometer (QTOF–MS/MS). Peptide LC–MS/MS data were processed by searching all MS^2 spectra against an in silico peptide library generated from protein-coding genes in a Chocolate Pots Metagenomic data set (Inskeep et al., 2013; Klatt et al., 2013). Relative phylogenetic abundances in each well were estimated by comparing the mean peptide intensities for proteins taxonomically assigned to a given phylogenetic group (defined in Table S2) to the sum of mean peptide intensity for all proteins in a given well (Mohr et al., 2014). This label-free protein quantification method is only semiquantitative, as are most label-free protein quantification methods (Bubis et al., 2017). Nonetheless, this quantification method was evaluated using a mixture of organisms of known quantity and found to have a $\pm 20\%$ root-mean-square error (Figure S12 from Mohr et al., 2014).

2.5 | Sugar extraction and derivatization

Extracellular polymeric substances (EPS) were extracted using a modified version of “method 8” as described in (see Table 1 from Klock et al., 2007). Briefly, 20 ml of 10% (w/v) NaCl was added to 10 grams of wet homogenized microbial mat sample and vortexed. This solution was incubated at 40°C for 15 min, followed by centrifugation at $8200g$ for 15 min. The supernatant was collected, and the precipitant was re-extracted with 20 ml 10% NaCl two more times. After cooling in an ice bath, 100% ethanol was added to the supernatant to a final concentration of 70%. EPS was precipitated at 4°C overnight and removed by centrifugation.

Extracted EPS were hydrolyzed into monomers using established methods (van Dongen et al., 2001). Briefly, the EPS were vortexed with 1 ml $12 \text{ M H}_2\text{SO}_4$ in a Teflon tube. A stir-bar was added, and the solution was stirred at ~ 400 rpm for 2 hr at room temperature, followed by dilution to 1 M and heating at 85°C for 4.5 h. After cooling

TABLE 1 Summary of $\delta^{13}\text{C}$ values for Chocolate Pots (CP) microbial mats

	$\delta^{13}\text{C}$ (‰)
Total organic carbon	-27.0 ± 0.1
Weighted average FA	-33.6 ± 0.3
Average protein	-25.4 ± 1.0
Glucose (EPS)	-25.1 ± 0.8

to room temperature, the solution was neutralized to pH 7 using BaCO_3 . Once neutralized, the solution was centrifuged at $4000g$ for 5 min, after which the supernatant was collected, frozen, and lyophilized.

Lyophilized sugar monomers were derivatized immediately prior to isotope analysis, again using established protocols (van Dongen et al., 2001). Arabinose, xylose, glucose, and myo-inositol standards with known $\delta^{13}\text{C}$ compositions (-11.7‰ , -9.7‰ , -11.1‰ , and -14.4‰ , respectively) were prepared in parallel to correct for the ^{13}C content of the carbon introduced during derivitization. Briefly, 1 ml of a methylboronic acid/pyridine (10 mg/ml) mixture was added to 5 mg of lyophilized sample or to 1 mg of total glucose, arabinose, and xylose standards and then heated at 60°C for 30 min, followed by the addition of $100 \mu\text{l N,O-bis}(\text{trimethylsilyl})\text{trifluoroacetamide}$ (BSTFA) and a further 5 min of heating. Because myo-inositol is insoluble in pyridine, $250\text{--}500 \mu\text{g}$ myo-inositol was instead dissolved in 1 ml dimethyl sulfoxide (DMSO) for derivitization. After the heating step, the myo-inositol standard mixture was cooled to room temperature before adding 1 ml of cyclohexane and $100 \mu\text{l}$ of BSTFA (Leblanc & Ball, 1978). All samples were dried under N_2 and quantitatively dissolved in ethyl acetate prior to isotope analysis.

2.6 | Isotope ratio mass spectrometry

To measure the $\delta^{13}\text{C}$ value of bulk total organic carbon (TOC), approximately 7.5 mg of triplicate freeze-dried microbial mat samples was placed in silver capsules (Costech) and acidified with $100 \mu\text{l}$ of 1 N HCl to remove dissolved inorganic carbon. Samples were dried at 50°C , enveloped in tin capsules (Costech), and analyzed on a Costech 4010 Elemental Analyzer connected to a Thermo Scientific Delta V IRMS (isotope ratio mass spectrometer).

Fatty acid methyl ester (FAME) and derivatized sugar monomer $\delta^{13}\text{C}$ compositions were analyzed via gas chromatography–isotope ratio mass spectrometry (GC–IRMS; Thermo Scientific Delta V Advantage connected to a Trace GC Ultra via a GC Isolink interface). In both cases, $1 \mu\text{l}$ of sample was co-injected with $0.5 \mu\text{l}$ of internal standard ($n\text{-C}_{32}$; $50 \text{ ng}/\mu\text{l}$). FAMES were run on a $30 \text{ m} \times 0.25 \text{ mm}$ HP-5MS column as previously described (Close et al., 2014). Sugar monomers were run on a $30 \text{ m} \times 0.25 \text{ mm}$ DB-1701 column; samples were transferred onto the column using a programmable temperature vaporizer (PTV) inlet at an injection temperature of 70°C followed by 330°C for 4 min. The GC–IRMS oven temperature gradient was adopted from van Dongen et al. (2001).

Stable carbon isotope analysis was conducted using spooling-wire microcombustion (SWiM)-IRMS (Caimi & Brenna, 1993; Brand & Dobberstein, 1996; Sessions et al., 2005; Thomas et al., 2011). The SWiM-IRMS configuration used here is adapted from Sessions et al. (2005) and is detailed in Mohr et al. (2014). Fractions (96-well plate aliquots) were measured in triplicate. Only data from wells containing $>0.56 \text{ nmol C}/\mu\text{l}$ ($\sim 350 \text{ mV}$ peak amplitude, m/z 44) and with measurement standard deviations $<2\%$ were retained (Mohr et al., 2014).

2.7 | Data analysis

Protein phylogenetic data were grouped into three taxonomic bins: Cyanobacteria + "other," Chloroflexi, and putative heterotrophs (Table S1). Estimates of the $\delta^{13}\text{C}$ compositions of proteins for each group (δ_{cyano} , δ_{chloro} , and δ_{het} , respectively) were calculated via three different methods using the measured $\delta^{13}\text{C}$ compositions (δ_m ; Table S4) and the estimated relative taxonomic abundances in each well.

The first method ($>95\%$ Unique) calculates the values of δ_{cyano} , δ_{chloro} , and δ_{het} from the average δ_m for only those wells in which $>95\%$ of the peptide signal intensity was assigned to just one of the three taxonomic groups. Precision for this method is reported as ± 1 SD from the mean. For the second (2-Component Mixture) and third (Linear Regression) methods, the δ_m values and estimated fractional abundances (from peptide signal intensity) were used in three over-determined linear equations:

$$\delta_{m,i} = \left(\sum \text{Pep}_{\text{cyano},i} \times \delta_{\text{cyano}} + \sum \text{Pep}_{\text{chloro},i} \times \delta_{\text{chloro}} \right) / \sum \text{Pep}_{\text{total}} \quad (1)$$

$$\delta_{m,i} = \left(\sum \text{Pep}_{\text{cyano},i} \times \delta_{\text{cyano}} + \sum \text{Pep}_{\text{chloro},i} \times \delta_{\text{chloro}} + \sum \text{Pep}_{\text{het},i} \times \delta_{\text{het}} \right) / \sum \text{Pep}_{\text{total}} \quad (2)$$

$$\delta_{m,i} / \sigma_{m,i} = \left(\sum \text{Pep}_{\text{cyano},i} \times \delta_{\text{cyano}} + \sum \text{Pep}_{\text{chloro},i} \times \delta_{\text{chloro}} + \sum \text{Pep}_{\text{het},i} \times \delta_{\text{het}} \right) / \left(\sum \text{Pep}_{\text{total}} \times \sigma_{m,i} \right) \quad (3)$$

where δ_{cyano} , δ_{chloro} , and δ_{het} are the unknowns, $\sum \text{Pep}$ is the summed QTOF-MS/MS ion counts for peptides, σ_m is the precision for δ_m (± 1 SD), and i is each individual plate well for which both δ_m and peptide signal intensities were measured (Mohr et al., 2014).

The 2-Component Mixture method uses Equation 1 to estimate δ_{cyano} and δ_{chloro} using wells in which peptides were detected only for the Cyanobacteria and Chloroflexi taxonomic groups. Endmembers were estimated via a Deming least-squares regression as detailed previously (Mohr et al., 2014). Deming least-squares regression minimizes the variance in both x and y , accounting for errors in both the independent variable (x) and the dependent variable (y) (Deming, 1943). Precision for this method is reported as the square root of the error variance.

The Linear Regression method uses Equations 2 and 3 to estimate δ_{cyano} , δ_{chloro} , and δ_{het} for the full data set. Equation 2 represents an unweighted estimate. Equation 3 is weighted by the precision

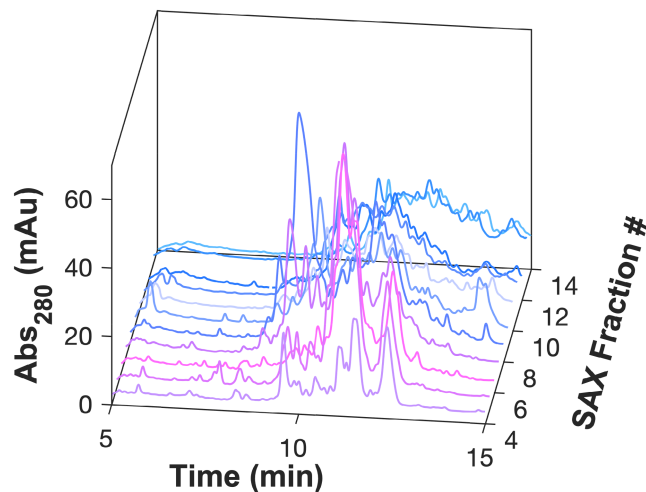


FIGURE 2 Reverse-phase (RP)-HPLC chromatograms of the spectral absorbance at 280nm for individual strong anion exchange (SAX fractions) S4-S14. Chromatogram color represents the visible color of each fraction (legend, top right; also see Figure S1)

of the isotopic measurements for each well (Glover et al., 2011). Equations 2 and 3 were solved inversely for δ_{cyano} , δ_{chloro} , and δ_{het} by singular value decomposition (SVD) using the built-in Matlab SVD function (Glover et al., 2011). Precision for this method is reported as \pm the square root of the error variance.

Individual amino acids (AAs) within organisms have different $\delta^{13}\text{C}$ values (Abelson & Hoering, 1961; Blair et al., 1985; Macko et al., 1987). However, the $\delta^{13}\text{C}$ compositions of average proteins are remarkably consistent (Hayes, 2001). To examine whether AA composition could be responsible for the observed isotopic differences between wells, we used the full AA sequences of our named proteins to determine the relative proportion of individual AAs in each analyzed sample. The distributions of individual AAs were then compared to the $\delta^{13}\text{C}$ composition of the wells containing that AA.

3 | RESULTS

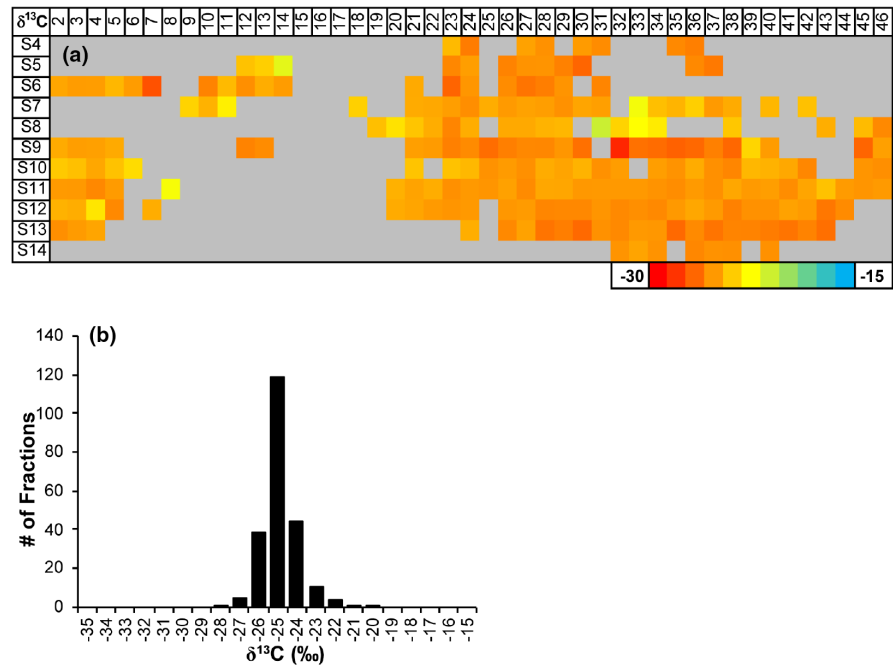
3.1 | Multidimensional protein chromatography

The 20 initial chromatographic (SAX) fractions of the bulk protein extract had distinct colors (Figure 2, Figure S1) reflecting the presence of chlorophyll a, phycobilin, and bacteriochlorophyll (c and a) pigments associated with photosynthetic proteins (Pierson & Parenteau, 2000). Further separation by RP-HPLC resulted in distinct chromatograms for each SAX fraction (Figure 2), consistent with the theoretical average resolving power of ca. 10^3 proteins for P-SIF chromatography (Mohr et al., 2014). SAX fractions 4-14 were chosen for further analysis using the integrated spectral absorbance of the RP-HPLC signal at 280nm and criteria from prior work (Mohr et al., 2014).

TABLE 2 Estimates of the $\delta^{13}\text{C}$ values (‰) of proteins for microbial groups from the Chocolate Pots (CP) mat as calculated from Protein Stable Isotope Fingerprinting (P-SIF) data using four different methods

Microbial group	>95% unique	2-component mixing	Weighted linear regression	Unweighted linear regression
Cyanobacteria + Other	-25.3 ± 0.7	-25.6 ± 0.6	-25.4 ± 0.2	-25.5 ± 0.3
Chloroflexi	-23.5 ± 1.8	-22.7 ± 0.6	-23.1 ± 0.5	-24.0 ± 0.5
Heterotrophs	-25.3 ± 0.7		-25.5 ± 0.7	-25.4 ± 0.6

FIGURE 3 (a) $\delta^{13}\text{C}$ values of individual reverse-phase (RP) chromatographic time slices (2–46) of strong anion exchange (SAX) fractions S4–S14. Gray areas indicate no usable data ($<0.56 \text{ nmol C}/\mu\text{l}$ and/or triplicate SD $> 2\%$). (b) Histogram of $\delta^{13}\text{C}$ values for SAX fractions shown in 3A. Values are not normally distributed (Shapiro–Wilk test, $p < 0.01$)



3.2 | Protein taxonomic identifications

Fifty percent (265/528) of the RP-HPLC fractions contained classifiable peptide sequences, yielding 277 unique proteins (Table S1): 170 proteins assigned to Cyanobacteria, 65 to Chloroflexi, 7 to Chlorobi, and all others (35 proteins) assigned to microbial groups containing four or fewer unique protein hits or to unclassified sources (Table S2). The mean and median number of unique peptides used to classify each protein were 4 and 3, respectively. Using the summed mean intensity of peptides assigned to proteins, we estimate the relative abundance of microbial groups to be 78.6% Cyanobacteria, 12.0% Chloroflexi and Chlorobi (11.6% Chloroflexi, 0.4% Chlorobi), and 9.4% other, which includes 5.1% putatively heterotrophic taxa and 4.3% unclassified (Table S2). The ordering of these data differs from the phylogenetic distribution of best Basic Local Alignment Search Tool (BLAST) hits for protein-coding genes in the CP metagenome, of which 49.7% were assigned to Chloroflexi, 28.1% to Cyanobacteria, 22.0% to heterotrophic organisms, and 0.2% to Chlorobi (Inskeep et al., 2013; Klatt et al., 2013). In contrast, the distribution of nearly full-length 16S ribosomal RNA (rRNA) gene sequences in the CP metagenome (42% assigned to Cyanobacteria, 28% to Chloroflexi, 7% to Chlorobi, 13% to heterotrophic organisms, and 10% unclassified), and the relative abundances of single-copy marker genes from

the metagenome assigned using AMPHORA (automated pipeline for phylogenomic analysis) both agree with the ordering of our relative abundance estimates (Inskeep et al., 2013; Klatt et al., 2013). The variability in relative abundances as estimated by these data is unsurprising, given that label-free protein quantification methods are only semiquantitative (Bubis et al., 2017) and copy numbers of 16s rRNA genes in particular are variable among bacterial phyla (Větrovský & Baldrian, 2013). More generally, the samples were taken seven years apart in two different months (August vs. October). At CP, the measured pH, concentrations of inorganic constituents, and vent-water temperatures have been remarkably consistent over 80 years (see Table 2 from Parenteau & Cady 2010). (Ferris & Ward, 1997) report a relatively little change in microbial community composition at Octopus Springs in YNP over an annual cycle; nonetheless, the difference in solar flux at this latitude between August and October may contribute to temporal shifts in microbial community composition (Ruff-Roberts et al., 1994). Additionally, our data represent the relative contributions by different microbial groups to total protein biomass, which may differ from the relative abundances of individual organisms. For example, Finkel et al. (2016) estimate a median 43.1% dry weight protein content in Cyanobacteria relative to a 27.4% dry weight protein content in diatoms. Mohr et al. (2014) calculated a $\pm 20\%$ root-mean-square error for P-SIF abundance estimates by

analysis of known mixtures of cultured organisms (Figure S12 from Mohr et al., 2014). Since the difference in relative abundance between Cyanobacteria and all other groups is more than 3 times this $\pm 20\%$ root-mean-square error, we are confident that our method effectively distinguishes between the dominant autotrophic organisms and heterotrophic organisms in our sample. The relative abundance of Chloroflexi (Table S2) is supported by prior reports that the former are the predominant anoxygenic phototrophs in circumneutral to alkaline hot springs in YNP (Bennett et al., 2020; Hamilton et al., 2019).

3.3 | Protein carbon isotopic compositions

Forty-two percent (224/528) of the RP-HPLC fractions contained enough carbon for isotopic measurement. Of these, 83% (186/224) had standard deviations $< 2.0\%$ and were used in subsequent analyses. The resulting protein fraction $\delta^{13}\text{C}$ values (Figure 3a; Table S4) were not normally distributed (Shapiro-Wilk test, $p < 0.01$) with a mean of -25.4% (Table 1, Figure 3b). The data show a moderately positive skew (skewness = 1.0), indicating a small but statistically significant contribution of isotopically more positive proteins.

The average standard deviation of triplicate $\delta^{13}\text{C}$ measurements for protein fractions was 0.6% for the whole data set, and 0.4% for the most abundant 50% as determined by the IRMS peak area (Table S3). These values represent average measurement errors lower than the population standard deviation (1.0%), indicating some degree of true variability among the protein $\delta^{13}\text{C}$ values (Table S3).

There were no statistically significant ($p = < 0.05$, Student's *t*-test) correlations between the relative distribution of individual AAs and the $\delta^{13}\text{C}$ values in each well (Table S6).

3.4 | Estimates of protein $\delta^{13}\text{C}$ values for microbial groups

Four different methods – (i) unique proteins, (ii) 2-component mixing, (iii) abundance-weighted multiple linear regression, and (iv) unweighted multiple linear regression – were used to estimate the $\delta^{13}\text{C}$ values of proteins originating from different microbial groups (Table 2, Figure 4). The results from all three approaches agree within 1% and indicate that Cyanobacteria and putatively heterotrophic organisms are isotopically indistinguishable, with mean estimates ranging from -25.6% to -25.3% . In contrast, the Chloroflexi are relatively ^{13}C -enriched, at -24.0% to -22.7% , depending on the estimation approach. Other taxonomic groups yielded too few assigned data points to resolve by mass-balance mixing approaches. However, in six wells, $> 45\%$ of the detected protein was classified as deriving from Actinobacteria, including one well apparently composed entirely of actinobacterial protein and having a $\delta^{13}\text{C}$ value of -25.1% . This value is indistinguishable within error from both the cyanobacterial and the heterotrophic mean values and is consistent

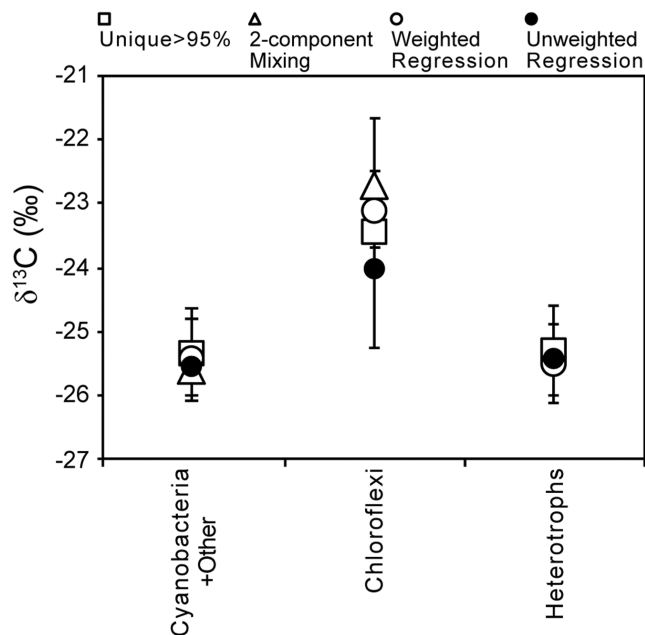


FIGURE 4 Estimates of the $\delta^{13}\text{C}$ values of proteins from taxonomic groups as calculated by four independent methods: i) wells in which $> 95\%$ of detected proteins belonged only to the indicated group (squares); ii) 2-component end-member solution for wells in which $> 95\%$ of detected proteins belonged only to Cyanobacteria or Chloroflexi (triangles); iii) estimated from all taxonomic abundance and $\delta^{13}\text{C}$ data using an abundance-weighted multiple linear regression routine (unfilled circles); iv) estimated from all taxonomic abundance and $\delta^{13}\text{C}$ data using an unweighted multiple linear regression routine (filled circles); see Methods for details

with a relatively high abundance of Actinobacteria in the heterotrophic population.

We can compare these estimates for taxon-specific protein $\delta^{13}\text{C}$ compositions to biomarker $\delta^{13}\text{C}$ values reported by Parenteau (2007). Data from a CP sample collected from the same location as our 2014 sample in July 2005 include three wax ester compounds (average $\delta^{13}\text{C}$ composition of $-30.2\% \pm 0.8\%$), which are biomarkers for Chloroflexi and are typically approximately 2% depleted in ^{13}C relative to biomass (van der Meer et al., 2001). This suggests Chloroflexi biomass from the 2005 CP sample had a $\delta^{13}\text{C}$ composition of approximately -28.2% . The 2005 CP sample also includes the cyanobacterial biomarkers *n*-heptadecane and phytol ($\delta^{13}\text{C}$ compositions of $-39.4\% \pm 3.1\%$ and $-35.2\% \pm 0.7\%$, respectively), which are typically approximately 8% and 6% depleted in ^{13}C relative to biomass, respectively (Sakata et al., 1997). These data suggest Cyanobacterial biomass from the 2005 CP sample had a $\delta^{13}\text{C}$ composition of approximately $-31.4\% \pm 3.1\%$ or $-29.2\% \pm 0.7\%$. These values should only be taken as back-of-the-envelope estimates. Nonetheless, similarly to our protein $\delta^{13}\text{C}$ estimates, Chloroflexi biomass $\delta^{13}\text{C}$ composition as estimated by these particular biomarker compounds is approximately 1% – 3% heavier than cyanobacterial biomass, in agreement with our protein data from the 2014 CP sample.

3.5 | Bulk, fatty acid, and sugar carbon isotope ratios

Total organic carbon in this sample (TOC; $-27.0 \pm 0.1\%$; Table 1) was ^{13}C -depleted relative to previous measurements of bulk biomass carbon reported previously for Chocolate Pots *Synechococcus*-*Chloroflexi* mats ($-23.2 \pm 0.8\%$ in 2004 and $-25.8 \pm 0.5\%$ in 2005; Parenteau, 2007). This TOC value is 1.6‰ depleted in ^{13}C relative to average bulk protein, while the weighted average fatty acids (FAs) were 6.6‰ depleted in ^{13}C relative to TOC (Figure 5). The $\delta^{13}\text{C}$ of dissolved inorganic carbon (DIC) in the vent water above the mat was not measured at the time of sampling. However, given prior measurements in the same location ($-2.0\% \pm 0.1\%$ in 2004 and $-1.0\% \pm 0.1\%$ in 2005; Parenteau, 2007) and the narrow range in pH, bicarbonate concentrations, and temperatures at CP over 80 years (see Table 2 from Parenteau & Cady 2010), the TOC in our sample is approximately 25‰ to 26‰ depleted in ^{13}C relative to the assumed DIC. This fractionation is within the expected range for organisms using the Calvin-Benson-Bassham Cycle (pentose phosphate cycle) for autotrophic carbon fixation in the 50–60°C range (Havig et al., 2011), which is consistent with the relatively high abundance of Cyanobacteria.

Individual FAs $n\text{-C}_{16:0}$, $n\text{-C}_{18:0}$, $n\text{-C}_{18:1}$, and $n\text{-C}_{18:2}$ were the only quantitatively significant FAs recovered (Table 3), in agreement with

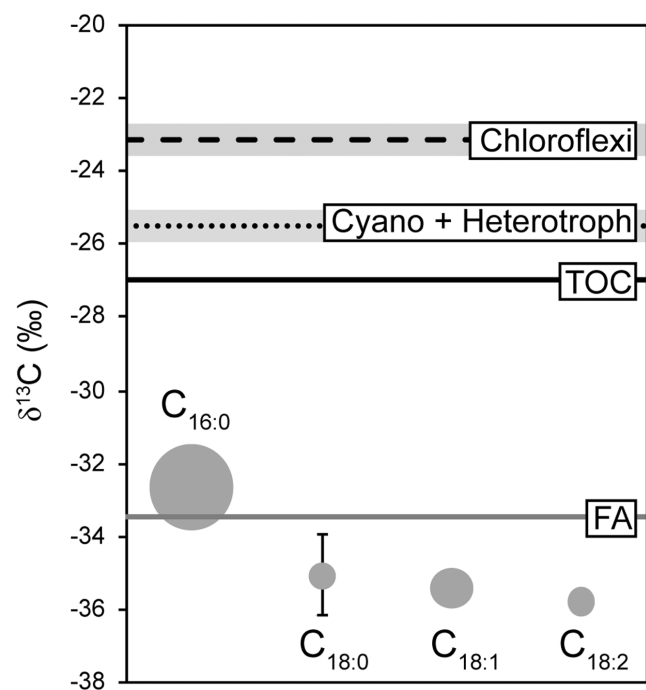


FIGURE 5 A composite of Chocolate Pots (CP) carbon isotopic data. Chloroflexi, Cyanobacteria, and heterotrophic protein $\delta^{13}\text{C}$ values are represented by dashed and dotted lines, respectively. The $\delta^{13}\text{C}$ value of total organic carbon (TOC) is shown in black. The weighted average fatty acid (FA) pool is shown in gray. The $\delta^{13}\text{C}$ values of individual FA are indicated by gray circles; circle area corresponds to abundance relative to the $n\text{-C}_{16:0}$ FA. Shading and error bars represent ± 1 SD from the mean

previous reports indicating these compounds comprise 93% of FAs in *Synechococcus*-*Chloroflexi* CP mats (Parenteau et al., 2014). The $\delta^{13}\text{C}$ values of these FAs ranged from 5.7 to 9.0‰ depleted in ^{13}C relative to TOC, equivalent to 7.3 to 10.6‰ depleted relative to average protein (Figure 5). This relative isotopic ordering also agrees with prior reports, where $n\text{-C}_{16:0}$, $n\text{-C}_{18:0}$, and $n\text{-C}_{18:1}$ FAs (average of phospholipid, neutral, and polar glycolipid FAs) had average $\delta^{13}\text{C}$ values that were 10.8‰, 12.1‰, and 12.8‰ offset from bulk biomass, respectively (Parenteau, 2007); their larger reported offsets are consistent with the more ^{13}C -enriched value reported for TOC in that earlier sample.

Glucose was the only quantitatively important sugar monomer recovered from extracted EPS. It had a $\delta^{13}\text{C}$ value of $-25.1\% \pm 0.8\%$ (Table 1), which is within error of the cyanobacterial and heterotrophic proteins as estimated by all methods (Table 2).

4 | DISCUSSION

4.1 | Cyanobacterial carbon production and excretion

In phototrophic microbial mats, cyanobacterial organic carbon is available to heterotrophic organisms as excreted carbon storage molecules, photorespiration by-products, fermentation products, or via viral lysis (Bateson & Ward, 1988; Carreira et al., 2015; Nold & Ward, 1996; Stal & Moezelaar, 1997). Under the high light intensity typical of the top layer of microbial mats, the supply rate of photons is likely to be less limiting than the supply rate of nutrients. Under these conditions, cyanobacteria allocate excess photosynthate to both stored and excreted molecules, primarily polysaccharides (Braakman et al., 2017; Fogg, 1983). This allows cyanobacteria to maintain a high carbon fixation rate (Fogg, 1983), manage adenosine triphosphate (ATP) levels (Cano et al., 2018), and store reduced carbon as an energy reserve for when light levels are low (Nold & Ward, 1996; Stal & Moezelaar, 1997). Cyanobacteria in a similar (48°C to 65°C) *Synechococcus*-*Chloroflexi* mat from Octopus Springs, YNP, allocated up to 85% of fixed CO_2 to polysaccharide (Nold & Ward, 1996). This ratio is in great excess of the typical molecular composition of cells (>30% protein for photosynthetic organisms; Finkel et al., 2016), implying the balance of this sugar production was excreted extracellularly. Cyanobacteria-derived polysaccharide forms the majority of EPS in microbial mats, and this material, after digestion by extracellular enzymes, is assimilated by heterotrophic organisms or reused by Cyanobacteria (Bateson & Ward, 1988; Flemming & Wingender, 2010; Klock et al., 2007; Stuart et al., 2016). In mats similar to CP, glucose-rich EPS is the most likely primary source of organic carbon for heterotrophs.

Previous studies on carbon transfer in YNP microbial mats have focused primarily on the uptake of fermentation products by FAPs (e.g., Bateson & Ward, 1988; Nold & Ward, 1996; van der Meer et al., 2003). To our knowledge, there is no work directly demonstrating the preferential uptake of EPS-derived carbohydrates (as

TABLE 3 $\delta^{13}\text{C}$ values for individual fatty acids (FAs) from Chocolate Pots (CP) microbial mats

FA	$\delta^{13}\text{C}$ (‰) ^a	Relative abundance
<i>n</i> -C _{16:0}	-32.7 ± 0.2	1
<i>n</i> -C _{18:0}	-35.1 ± 1.1	0.11
<i>n</i> -C _{18:1}	-35.4 ± 0.4	0.24
<i>n</i> -C _{18:2}	-35.8 ± 0.1	0.10

^aValues are averaged from triplicate (*n*-C_{16:0}) and duplicate (*n*-C_{18:x}) gas chromatography–isotope ratio mass spectrometry (GC-IRMS) runs.

opposed to their fermentation products) by heterotrophs in YNP subaerial mats. Stuart et al. (2016) characterized the exoproteome of both natural and cultured marine cyanobacterial mats and found that the majority of proteins in EPS were related to carbohydrate and amino-acid metabolism. Furthermore, the two most abundant heterotrophic phyla in our CP mat (Actinobacteria and Bacteroidetes) are known to assimilate and ferment glucose in culture (de Vos et al., 2009; Whitman et al., 2010).

We thus hypothesize that the isotopic similarity between Cyanobacteria and heterotrophs is due to the latter organisms directly consuming glucose-rich EPS excreted by the former. In support of this idea, the glucose moieties of EPS extracted from our CP sample are isotopically indistinguishable from the protein $\delta^{13}\text{C}$ values of both the Cyanobacteria and heterotrophs in the community. To our knowledge, there is only one prior report on the $\delta^{13}\text{C}$ composition of extracellular EPS in a microbial mat (rather than cell-associated sugar monomers), and in it, EPS again are isotopically equal to bulk organic carbon (Wieland et al., 2008).

Initially, both our findings here and the work of Wieland et al. (2008) appear to contradict prior work on the carbon isotopic composition of cell-associated glucose monomers (Teece & Fogel, 2007; van der Meer et al., 2003; van Dongen et al., 2002). In these reports, glucose monomers extracted from cells were enriched in ^{13}C relative to bulk biomass. However, this pattern excludes glucose from a cyanobacterial culture, which is depleted in ^{13}C relative to cyanobacterial biomass (Teece & Fogel, 2007). In either case, we can resolve this discrepancy by differentiating between internal (cell-associated) and external (EPS) sugars. Pereira et al. (2009) note that differences in the $\delta^{13}\text{C}$ compositions of internal hexose monomers in Cyanobacteria are likely due to isotopic fractionation during the polymerization of internal sugars to polysaccharide. Enzymatic products are typically depleted in ^{13}C relative to reactants. As such, EPS are likely depleted in ^{13}C relative to the internal pool of free sugars from which they are polymerized. Furthermore, because subaerial mat-forming Cyanobacteria allocate the majority of their fixed carbon to polysaccharides, we assume the expressed fractionation is minimal and the polysaccharide fraction (the dominant product) should isotopically resemble the initial photosynthate (Hayes, 2001).

In summary, cyanobacterial and heterotrophic proteins are isotopically indistinguishable because both organisms are utilizing simple sugars derived from cyanobacterial photosynthate as their anabolic

carbon source. At the broader level, a hypothesis of near-zero ^{13}C fractionation by organisms growing on pure sugar substrates is consistent with some of the earliest works of stable isotope biogeochemistry: *Chlorella pyrenoidosa* biomass was isotopically indistinguishable from the glucose substrate (Abelson & Hoering, 1961), while *Escherichia coli* biomass was depleted in ^{13}C relative to glucose substrate (Abelson & Hoering, 1961; Blair et al., 1985). The ^{13}C -depletion in the latter organism may be understood as a reflection of total biomass (i.e., including its ^{13}C -depleted lipid component), while lack of a significantly ^{13}C -depleted bulk signal in *Chlorella* may reflect a smaller fractional contribution of lipids to the bulk cell.

4.2 | Chloroflexi carbon sources

Chloroflexi can grow photoautotrophically (*Chloroflexus* spp.) via the anoxygenic 3-hydroxypropionate (3-HP) pathway, photoheterotrophically under light anoxic conditions (all FAPs) via the assimilation of low-molecular-weight organic compounds (Bauld & Brock, 1973; Giovannoni et al., 1987; Hanada et al., 2002; van der Meer et al., 2010; Zarzycki & Fuchs, 2011), or photomixotrophically by simultaneously incorporating inorganic and organic carbon sources (*Chloroflexus*, *Roseiflexus*) (Klatt et al., 2013). Chloroflexi can also grow heterotrophically under dark aerobic conditions. When grown purely photoautotrophically, the biomass of *Chloroflexus aurantiacus* is ~13‰ depleted in ^{13}C relative to the carbon source (van der Meer et al., 2001; House et al., 2003). Using our estimate for Chloroflexi biomass (-23.1 ± 0.5‰), a $\delta^{13}\text{C}$ value of -1.0‰ ± 0.1‰ for CP dissolved inorganic carbon (Parenteau, 2007), an assumed photoautotrophic Chloroflexi biomass maximum value of -14.0‰ ± 0.1‰ (van der Meer et al., 2001), and our estimated heterotrophic endmember (-25.4‰ ± 0.2‰), isotope mass balance implies the FAPs obtain 20% ± 4% of their carbon autotrophically and the remaining ~80% by heterotrophic assimilation (if the latter substrate is sugar, or isotopically identical to sugar).

A recent report of in situ rates of anoxygenic photosynthesis across a broad range of mat systems in YNP mentions that anoxygenic photoautotrophy was not detected in sites below pH 6; however, the same authors report the presence and transcripts of *bchY* genes (which are considered markers for anoxygenic photosynthesis, see Hamilton et al., 2012) at these sites, supporting active photoheterotrophy (Hamilton et al., 2019). While our CP sample was collected at pH 6.1, historical measurements have measured a range of pH 5.7–6.1, placing CP directly on this threshold and supporting primarily (but not necessarily exclusively) photoheterotrophic growth by Chloroflexi at CP (Parenteau & Cady 2010). In the present work, we do not distinguish between individual taxa of Chloroflexi. Bennett et al. (2020) report bulk biomass $\delta^{13}\text{C}$ values similar to autotrophic *C. aurantiacus*, and they find more abundant Chloroflexus operational taxonomic units (OTUs) and relatively heavier bulk $\delta^{13}\text{C}$ values at alkaline sites below 59.3°C than sites above 59.3°C. In contrast, *Roseiflexus* OTUs were most abundant between 58.3°C and 71.8°C (Bennett et al., 2020). It is thus possible that our sample

represents a relatively larger contribution of *Roseiflexus*, albeit from a relatively acidic (pH 6.1) and cooler (49.7°C) site compared to those from Bennett et al. (2020).

Both laboratory culture and in situ studies support the idea that phototrophic Chloroflexi favor predominantly photoheterotrophic growth. In laboratory culture, the fastest growth rates for *C. aurantiacus* and two strains of *Roseiflexus* are observed in media supplemented with organic carbon substrates (Bauld & Brock, 1973; Giovannoni et al., 1987; Hanada et al., 2002; van der Meer et al., 2010; Zarzycki & Fuchs, 2011). Attempts to grow *Roseiflexus* photoautotrophically in culture have been unsuccessful (Hanada et al., 2002; van der Meer et al., 2010), although it does contain the genes for the 3-HP pathway (Klatt et al., 2007), and has been shown to grow photoautotrophically and/or photomixotrophically in situ (Klatt et al., 2013). *Chloroflexus* can be cultured both autotrophically and heterotrophically (when photoautotrophy is inhibited) via the glyoxylate cycle, but these modes have slower growth rates (Giovannoni et al., 1987; Pierson & Castenholz, 1974; Zarzycki & Fuchs, 2011). The pervasiveness of photoheterotrophic growth hypothesized by these culture studies is corroborated in situ via isotope-labeling experiments that show incorporation of labeled organic compounds by Chloroflexi in microbial mat environments; in particular, multiple studies point to the incorporation of fermentation products (e.g., acetate) in microbial mats (Anderson et al., 1987; Nold & Ward, 1996; van der Meer et al., 2005).

Therefore, an alternate explanation is that the phototrophic Chloroflexi in the CP mat may be growing nearly completely photoheterotrophically and are accessing a distinct carbon pool (with a different $\delta^{13}\text{C}$ value) than the other CP heterotrophs. While measurements of the $\delta^{13}\text{C}$ composition of bacterial fermentation products are scarce, acetate produced via fermentation by *E. coli* and *Clostridium papyrosolvens* is ^{13}C -enriched relative to source glucose (Blair et al., 1985; Penning & Conrad, 2006). Given the metabolic flexibility of the phototrophic Chloroflexi, the CP community may grow photoheterotrophically on acetate and/or partially photoautotrophically, in addition to a generally high background rate of sugar-driven heterotrophy.

4.3 | Comparison to lipid $\delta^{13}\text{C}$

Lipids and pigments are organic compounds that have a high preservation fidelity in the sedimentary record (Luo et al., 2019). Contextualizing $\delta^{13}\text{C}$ values of ancient lipid biomarkers requires estimating the difference in $\delta^{13}\text{C}$ values between lipids and biomass ($\epsilon_{\text{bio-lipid}}$). Estimating $\epsilon_{\text{bio-lipid}}$ accurately requires knowing the proportion of fixed carbon allocated to lipids, which can change depending on nutrient and light availability (Hayes, 2001; Mouginito et al., 2015; Tibocha-Bonilla et al., 2020). Furthermore, $\epsilon_{\text{bio-lipid}}$ differs in heterotrophic organisms grown on glucose versus acetate (Blair et al., 1985; DeNiro & Epstein, 1977; Tang et al., 2017).

Our phylum-specific protein $\delta^{13}\text{C}$ values allow calculation of the offset between FAs and specific microbial groups in our CP mats.

The 8.5–9.3‰ offset between TOC and the 18-carbon FAs is consistent with a dominantly cyanobacterial source, as the maximum $\epsilon_{\text{bio-lipid}}$ reported (~8–11‰) is unique to Cyanobacteria (Parenteau et al., 2014; Sakata et al., 1997). In particular, the 11‰ offset between the *n*-C_{18:2} FA and cyanobacterial protein is consistent with prior reports that this FA is primarily produced by Cyanobacteria (Kenyon et al., 1972; Parenteau et al., 2014).

The relatively large $\epsilon_{\text{bio-lipid}}$ estimated for Cyanobacteria in CP is consistent with our hypothesis that Cyanobacteria are allocating the majority of fixed carbon to storage sugars. When only a small proportion of the initial C₃ monomers of photosynthesis are decarboxylated to acetate, this enables greater expression of the isotope effect of pyruvate dehydrogenase (DeNiro & Epstein, 1977). Accordingly, $\epsilon_{\text{bio-lipid}}$ increases both due to this greater expression of the isotopic fractionation for lipid synthesis and because the bulk cell is composed of less lipid overall (Hayes, 2001; Sakata et al., 1997).

4.4 | Implications for the geologic record

Microbial mat environments were likely widespread during the Proterozoic and early Paleozoic (Callow & Brasier, 2009; Gehling, 1999; Hagadorn & Bottjer, 1997; Steiner & Reiter, 2001; Tarhan, 2018). As such, interpreting the $\delta^{13}\text{C}$ values of well-preserved organic matter from Proterozoic sediments requires understanding the isotopic consequences of carbon transfer within microbial mats specifically. Unlike water-column heterotrophs feeding on “marine snow,” which is a diverse assemblage of organic compounds of various classes (Alldredge & Silver, 1988), our data indicate that heterotrophs in subaerial or shallow, highly photic mats are consuming photosynthetic sugars. This ecosystem represents both production and consumption dominated by aerobic metabolisms (oxygenic photosynthesis and aerobic respiration). We therefore would predict this pattern to be widespread in post-GOE (Great Oxidation Event) surface environments, in which oxygenic Cyanobacteria came to dominate under conditions of high light intensity and/or low nutrient availability (Crockford et al., 2018; Havig et al., 2017; Reinhard et al., 2017). Any such system may allocate the majority of initial photosynthate to storage sugars (Fogg, 1983). If such mat environments were common during the Proterozoic and early Paleozoic, “you are what you eat”, rather than “you are what you eat, +1‰” is more likely to apply to those environments. The corollary to such an assertion is that systematic ^{13}C enrichment in bulk TOC, either on its own or relative to various biochemical fractions (e.g., Close et al., 2011; Logan et al., 1995; Pawlowska et al., 2013), would instead represent either a diagenetic signal (Cheng et al., 2015; Tang et al., 2005; Vinnichenko et al., 2021), a relatively greater assimilation of ^{13}C -enriched substrates like acetate (Blair et al., 1985; Penning & Conrad, 2006), or a complex mixture of alternative metabolisms (Havig et al., 2017 and references therein) (including overprinting by other anaerobic degradation pathways in addition to acetate fermentation).

Contrary to biochemical expectations, straight-chain lipids extracted from Proterozoic sediments are consistently ^{13}C -enriched relative to kerogen (Hayes, 2001; Logan et al., 1995). Initially, this inversion was attributed to the selective preservation of lipids from benthic heterotrophs assimilating organic carbon which, due to the slower sinking rate of Proterozoic organic matter, was subject to multiple rounds of remineralization in the water column (Logan et al., 1995). This hypothesis assumes that heterotrophic biomass becomes isotopically more positive per trophic level. It further requires that water-column remineralization is intense enough to enrich lipids in ^{13}C while both (1) preserving sufficient heterotrophic lipid to form the majority of the preserved lipid pool and (2) degrading sufficient heterotrophic biomass such that primary biomass forms the majority of the kerogen pool (Close et al., 2011). While such conditions are predicted to occur only rarely, if ever, within the water column (Close et al., 2011), some have suggested that these conditions are possible within microbial mats (Jahnke & des Marais, 2019; Pawlowska et al., 2013).

The absence of any distinguishable $\delta^{13}\text{C}$ signatures associated with heterotrophy in the subaerial CP *Synechococcus*-*Chloroflexi* mat suggests that the prevalence of microbial mat environments during the Proterozoic is not the sole explanation for the isotopic inversion between *n*-alkyl lipids and kerogen observed in rocks of Proterozoic age. Recent work favors a diagenetic source for the inversion. Samples from the Paleoproterozoic Barney Creek Formation have a relatively constant $\delta^{13}\text{C}$ composition of kerogen, while the $\delta^{13}\text{C}$ values of *n*-alkanes increase by 6.8‰ on average and are correlated with increasing thermal maturity (Vinnichenko et al., 2021). These data are supported by experiments on crude oil and Paleogene source rocks where the $\delta^{13}\text{C}$ compositions of *n*-alkanes increased by approximately 3–6‰ after undergoing artificial maturation (Cheng et al., 2015; Tang et al., 2005; Tian et al., 2017), as well as by Phanerozoic field-based studies that show equivalent increases of approximately 2–4‰ (Clayton & Bjorøy 1994; Dawson et al., 2007; Odden et al., 2002; Cheng et al., 2015). Low-molecular-weight (< C_{19}) compounds can be enriched in ^{13}C by up to 4‰ relative to crude oil after biodegradation (Pedentchouk & Zhou, 2020; Sun et al., 2005). However, Vinnichenko et al. (2021) dismiss the effects of biodegradation on the $\delta^{13}\text{C}$ compositions of *n*-alkanes in their samples due to the constant relative abundances of *n*-alkanes in the samples. Furthermore, diagenesis on its own does not explain the relative lack of inverted isotope signal throughout the Phanerozoic (Logan et al., 1995). While this may partly reflect the greater availability of thermally immature sediments in the Phanerozoic combined with a researcher bias toward these sediments, it does not explain reemergence of unusual ^{13}C lipid ordering at the Permian–Triassic boundary coincident with extinction-associated ecosystem changes (Grice et al., 2005).

The only isotopically distinct group detected in the CP mat was the *Chloroflexi*, which can be attributed to either a bicarbonate-utilizing autotrophic metabolism (3-HP), the assimilation of low-molecular-weight compounds (e.g., acetate), or a combination of both signals. Molecular clock estimates suggest the 3-HP pathway

did not evolve until the end of the Proterozoic (Shih et al., 2017). Nonetheless, these results suggest that the $\delta^{13}\text{C}$ composition of microbial biomass is more closely tied to specific metabolites than to autotrophy versus heterotrophy. As such, interpretations of the $\delta^{13}\text{C}$ values in sediments derived from predominantly microbial ecosystems should be developed relative to the $\delta^{13}\text{C}$ values of specific molecular-level carbon sources.

5 | CONCLUSIONS

Here, the results from an oxygenic, photosynthetic microbial mat indicate that the protein subfractions of *Cyanobacteria* and obligate heterotrophs such as *Actinobacteria* have indistinguishable $\delta^{13}\text{C}$ signatures. Such ecosystems – specifically shallow or subaerial microbial mat environments – are dominated by oxygenic photosynthesis and aerobic, heterotrophic respiration. This suggests that sugar production and consumption dominate the net ecosystem metabolism, yielding a community in which producers and consumers share primary photosynthate as a common resource. Proteins assigned to the FAP bacteria from the phylum *Chloroflexi* (*Roseiflexus* sp. and *Chloroflexus* sp.) were approximately 2‰ enriched relative to both *Cyanobacteria* and other heterotrophs, indicating that they are growing partially photoautotrophically, or are consuming a carbon substrate (e.g., acetate) with a distinct isotopic composition. Our results caution against applying “you are what you eat, +1‰” to microbial community food webs, especially when interpreting $\delta^{13}\text{C}$ values of ancient sediments derived from predominantly microbial ecosystems such as microbial mats.

ACKNOWLEDGMENTS

We thank A. Sessions, P.R. Girguis, S. Shah, and S.J. Carter for analytical advice. This work was supported by grants from the Gordon and Betty Moore Foundation (to A.P.) by a Marie-Curie International Outgoing Fellowship (to W.M.), and by a National Science Foundation Graduate Research Fellowship (to A.G.).

CONFLICT OF INTEREST

The authors declare no conflict of interest.

DATA AVAILABILITY STATEMENT

The data that support the findings of this study are available in the supplementary material of this article.

ORCID

Ana C. Gonzalez-Nayek  <https://orcid.org/0000-0002-2306-845X>

Wiebke Mohr  <https://orcid.org/0000-0002-1126-1455>

Linda L. Jahnke  <https://orcid.org/0000-0001-7241-3603>

REFERENCES

Abelson, P. H., & Hoering, T. C. (1961). Carbon isotope fractionation in formation of amino acids by photosynthetic organisms. *Proceedings*

- of the National Academy of Sciences of the United States of America, 47, 623–632.
- Allredge, A. L., & Silver, M. W. (1988). Characteristics, dynamics and significance of marine snow. *Progress in Oceanography*, 20(1), 41–82.
- Anderson, K. L., Tayne, T. A., & Ward, D. M. (1987). Formation and fate of fermentation products in hot spring cyanobacterial mats. *Applied and Environmental Microbiology*, 53, 2343–2352.
- Arnosti, C., Steen, A. D., Ziervogel, K., Ghobrial, S., & Jeffrey, W. H. (2011). Latitudinal gradients in degradation of marine dissolved organic carbon. *PLoS One*, 6, 8–13.
- Awramik, S. M. (1992). The oldest records of photosynthesis. *Photosynthesis Research*, 33, 75–89.
- Bateson, M. M., & Ward, D. M. (1988). Photoexcretion and fate of glycolate in a hot spring cyanobacterial mat. *Applied and Environmental Microbiology*, 54, 1738–1743.
- Bauld, J., & Brock, T. D. (1973). Ecological studies of chloroflexis, a gliding photosynthetic bacterium. *Archiv für Mikrobiologie*, 92(4), 267–284.
- Bennett, A. C., Murugapiran, S. K., & Hamilton, T. L. (2020). Temperature impacts community structure and function of phototrophic chloroflexi and cyanobacteria in two alkaline hot springs in Yellowstone National Park. *Environmental Microbiology Reports*, 12, 503–513.
- Blair, N., Leu, A., Muñoz, E., Olsen, J., Kwong, E., & des Marais, D. (1985). Carbon isotopic fractionation in heterotrophic microbial metabolism. *Applied and Environmental Microbiology*, 50, 996–1001.
- Braakman, R., Follows, M. J., & Chisholm, S. W. (2017). Metabolic evolution and the self-organization of ecosystems. *Proceedings of the National Academy of Sciences*, 114, E3091–E3100.
- Brand, W. A., & Dobberstein, P. (1996). Isotope-ratio-monitoring liquid chromatography mass spectrometry (IRM-LCMS): First results from a moving wire interface system. *Isotopes in Environmental and Health Studies*, 32, 275–283.
- Breteler, W. C. K., Grice, K., Schouten, S., Kloosterhuis, H. T., & Damsté, J. S. S. (2002). Stable carbon isotope fractionation in the marine copepod *Temora longicornis*: Unexpectedly low $\delta^{13}\text{C}$ value of faecal pellets. *Marine Ecology Progress Series*, 240, 195–204.
- Bubis, J. A., Levitsky, L. I., Ivanov, M. V., Tarasova, I. A., & Gorshkov, M. V. (2017). Comparative evaluation of label-free quantification methods for shotgun proteomics. *Rapid Communications in Mass Spectrometry*, 31, 606–612.
- Cabana, G., & Rasmussen, J. B. (1996). Comparison of aquatic food chains using nitrogen isotopes. *Proceedings of the National Academy of Sciences of the United States of America*, 93, 10844–10847.
- Caimi, R., & Brenna, T. (1993). High-precision liquid chromatography-combustion isotope ratio mass spectrometry. *Analytical Chemistry*, 65, 3497–3500.
- Callow, R. H. T., & Brasier, M. D. (2009). Remarkable preservation of microbial mats in Neoproterozoic siliciclastic settings: Implications for Ediacaran taphonomic models. *Earth-Science Reviews*, 96, 207–219.
- Cano, M., Holland, S. C., Artier, J., Burnap, R. L., Ghirardi, M., Morgan, J. A., & Yu, J. (2018). Glycogen synthesis and metabolite overflow contribute to energy balancing in cyanobacteria. *Cell Reports*, 23(3), 667–672.
- Carreira, C., Staal, M., Middelboe, M., & Brussaard, C. P. D. (2015). Counting viruses and bacteria in photosynthetic microbial mats. *Applied and Environmental Microbiology*, 81, 2149–2155.
- Cheng, P., Xiao, X. M., Gai, H. F., Li, T. F., Zhang, Y. Z., Huang, B. J., & Wilkins, R. W. T. (2015). Characteristics and origin of carbon isotopes of n-alkanes in crude oils from the Western Pearl River Mouth Basin, South China Sea. *Marine and Petroleum Geology*, 67, 217–229.
- Clayton, C., & Bjørøy, M. (1994). Effect of maturity on $^{13}\text{C}/^{12}\text{C}$ ratios of individual compounds in North Sea oils. *Organic Geochemistry*, 21, 737–750.
- Close, H. G., Bovee, R., & Pearson, A. (2011). Inverse carbon isotope patterns of lipids and kerogen record heterogeneous primary biomass. *Geobiology*, 9, 250–265.
- Close, H. G., Wakeham, S. G., & Pearson, A. (2014). Lipid and ^{13}C signatures of submicron and suspended particulate organic matter in the eastern tropical North Pacific: Implications for the contribution of bacteria. *Deep-Sea Research Part I: Oceanographic Research Papers*, 85, 15–34.
- Crockford, P. W., Hayles, J. A., Bao, H., Planavsky, N. J., Bekker, A., Fralick, P. W., Halverson, G. P., Bui, T. H., Peng, Y., & Wing, B. A. (2018). Triple oxygen isotope evidence for limited mid-Proterozoic primary productivity. *Nature*, 559, 613–616.
- Dawson, D., Grice, K., & Alexander, R. (2007). The effect of source and maturity on the stable isotopic compositions of individual hydrocarbons in sediments and crude oils from the Vulcan sub-basin, Timor Sea. *Geochemistry*, 38(7), 1015–1038.
- DeNiro, M., & Epstein, S. (1978). Influence of diet on the distribution of carbon isotopes in animals. *Geochimica et Cosmochimica Acta*, 42, 495–506.
- de Vos P., Garrity G. M., Jones D., Krieg N. R., Ludwig W., Rainey F. A., Schleifer K.-H., Whitman W. B. (2009) *Bergey's manual of systematic bacteriology volume three the firmicutes*. Springer.
- Dekas, A. E., Parada, A. E., Mayali, X., Fuhrman, J. A., Wollard, J., Weber, P. K., & Pett-Ridge, J. (2019). Characterizing chemoautotrophy and heterotrophy in marine archaea and bacteria with single-cell multi-isotope NanoSIP. *Frontiers in Microbiology*, 10, 2682.
- Deming W. E. (1943) *Statistical adjustment of data*.
- DeNiro, M. J., & Epstein, S. (1977). Mechanism of carbon isotope fractionation associated with lipid synthesis. *Science*, 197, 261–263.
- Djokic, T., van Kranendonk, M. J., Campbell, K. A., Havig, J. R., Walter, M. R., & Guido, D. M. (2021). A reconstructed subaerial hot spring field in the *3.5 billion-year-old dresser formation, North Pole Dome, Pilbara Craton, Western Australia. *Astrobiology*, 21, 1–38.
- Fantle, M. S., Dittel, A. I., Schwalm, S. M., Epifanio, C. E., & Fogel, M. L. (1999). A food web analysis of the juvenile blue crab, *Callinectes sapidus*, using stable isotopes in whole animals and individual amino acids. *Oecologia*, 120, 416–426.
- Ferris, M. J., & Ward, D. M. (1997). Seasonal distributions of dominant 16S rRNA-defined populations in a hot spring microbial mat examined by denaturing gradient gel electrophoresis. *Applied and Environmental Microbiology*, 63, 1375–1381.
- Finkel, Z. V., Follows, M. J., Liefer, J. D., Brown, C. M., Benner, I., & Irwin, A. J. (2016). Phylogenetic diversity in the macromolecular composition of microalgae. *PLoS One*, 11, 1–16.
- Flemming, H. C., & Wingender, J. (2010). The biofilm matrix. *Nature Reviews Microbiology*, 8, 623–633.
- Fogg, G. E. (1983). The ecological significance of extracellular products of phytoplankton photosynthesis. *Botanica Marina*, 26, 3–14.
- Fry, B., & Sherr, E. B. (1984). Delta super ^{13}C measurements as indicators of carbon flow in marine and freshwater ecosystems. *Contributions in Marine Science*, 27, 13–47.
- Gehling, J. G. (1999). Microbial mats in terminal Proterozoic siliciclastics; Ediacaran death masks. *PALAIOS*, 14, 40–57.
- Giovannoni, S. J., Revsbech, N. P., Ward, D. M., & Castenholz, R. W. (1987). Obligately phototrophic chloroflexus: Primary production in anaerobic hot spring microbial mats. *Archives of Microbiology*, 147(1), 80–87.
- Glover, D. M., Jenkins, W. J., & Doney, S. C. (2011). *Modeling methods for marine science*. Cambridge University Press.
- Görke, B., & Stülke, J. (2008). Carbon catabolite repression in bacteria: Many ways to make the most out of nutrients. *Nature Reviews Microbiology*, 6(8), 613–624.
- Grice, K., Cao, C., Love, G. D., Böttcher, M. E., Twitchett, R. J., Grosjean, E., Summons, R. E., Turgeon, S. C., Dunning, W., & Jin, Y. (2005). Photic zone Euxinia during the Permian-Triassic Superanoxic event. *Science*, 307(5710), 706–709.
- Hagadorn, J. W., & Bottjer, D. J. (1997). Wrinkle structures: Microbially mediated sedimentary structures common in subtidal siliciclastic

- settings at the Proterozoic-phanerozoic transition. *Geology*, 25, 1047–1050.
- Hamilton, T. L., Vogl, K., & Peters, J. W. (2012). Environmental constraints defining the distribution, composition, and evolution of chlorophototrophs in thermal features of Yellowstone National Park. *Geobiology*, 10(3), 236–249.
- Hamilton, T. L., Bennett, A. C., Murugapiran, S. K., & Havig, J. R. (2019). Anoxygenic phototrophs span geochemical gradients and diverse morphologies in terrestrial geothermal spring. *mSystems*, 4, 1–25.
- Hanada, S., Takaichi, S., Matsuura, K., & Nakamura, K. (2002). Roseiflexus castenholzii gen. Nov., sp. nov., a thermophilic, filamentous, photosynthetic bacterium that lacks chlorosomes. *International Journal of Systematic and Evolutionary Microbiology*, 52, 187–193.
- Havig, J. R., Raymond, J., Meyer-Dombard, D. R., Zolotova, N., & Shock, E. L. (2011). Merging isotopes and community genomics in a siliceous sinter-depositing hot spring. *Journal of Geophysical Research: Biogeosciences*, 116, 1–15.
- Havig, J., Hamilton, T., Bachan, A., Kump, L. R., Havig, J. R., & Hamilton, T. L. (2017). Sulfur and carbon isotopic evidence for metabolic pathway evolution and a four-stepped earth system progression across the Archean and Paleoproterozoic. *Earth-Science Reviews*, 174, 1–21.
- Hayes, J. M. (2001). Fractionation of carbon and hydrogen isotopes in biosynthetic processes. *Reviews in Mineralogy and Geochemistry*, 43, 225–277.
- Hoffman, H. J. (2000). Archean stromatolites as microbial archives. In *Microbial Sediments*. Springer.
- House, C. H., Schopf, J. W., & Stetter, K. O. (2003). Carbon isotopic fractionation by Archaeans and other thermophilic prokaryotes. *Organic Geochemistry*, 34(3), 345–356.
- Inskeep, W. P., Jay, Z. J., Tringe, S. G., Herrgård, M. J., & Rusch, D. B. (2013). The YNP metagenome project: Environmental parameters responsible for microbial distribution in the yellowstone geothermal ecosystem. *Frontiers in Microbiology*, 4, 67.
- Jahnke, L. L., & des Marais, D. J. (2019). Carbon isotopic composition of lipid biomarkers from an endoevaporitic gypsum crust microbial mat reveals cycling of mineralized organic carbon. *Geobiology*, 17, 643–659.
- Jahnke, L., Embaye, T., Hope, J., Turk, K. A., van Zuilen, M., des Marais, D. J., Farmer, J. D., & Summons, R. E. (2004). Lipid biomarker and carbon isotopic signatures for stromatolite-forming, microbial mat communities and Phormidium cultures from Yellowstone National Park. *Geobiology*, 2, 31–47.
- Kenyon, C. N., Rippka, R., & Stanier, R. Y. (1972). Fatty acid composition and physiological properties of some filamentous blue-green algae. *Archiv für Mikrobiologie*, 83(3), 216–236.
- Klatt, C. G., Bryant, D. A., & Ward, D. M. (2007). Comparative genomics provides evidence for the 3-hydroxypropionate autotrophic pathway in filamentous anoxygenic phototrophic bacteria and in hot spring microbial mats. *Environmental Microbiology*, 9(8), 2067–2078.
- Klatt, C. G., Inskeep, W. P., Herrgard, M. J., Jay, Z. J., Rusch, D. B., Tringe, S. G., Parenteau, M. N., Ward, D. M., Boomer, S. M., Bryant, D. A., & Miller, S. R. (2013). Community structure and function of high-temperature chlorophototrophic microbial mats inhabiting diverse geothermal environments. *Frontiers in Microbiology*, 4, 106.
- Kleiner, M., Dong, X., Hinzke, T., Wippler, J., Thorson, E., Mayer, B., & Strous, M. (2018). Metaproteomics method to determine carbon sources and assimilation pathways of species in microbial communities. *Proceedings of the National Academy of Sciences of the United States of America*, 115, E5576–E5584.
- Klock, J. H., Wieland, A., Seifert, R., & Michaelis, W. (2007). Extracellular polymeric substances (EPS) from cyanobacterial mats: Characterisation and isolation method optimisation. *Marine Biology*, 152, 1077–1085.
- Leblanc, D. J., & Ball, A. J. S. (1978). A fast one-step method for the silylation of sugars and sugar phosphates. *Analytical Biochemistry*, 84, 574–578.
- Logan, G. A., Hayes, J. M., Hieshima, G. B., & Summons, R. E. (1995). Terminal Proterozoic reorganization of biogeochemical cycles. *Nature*, 376, 53–56.
- Luo, G., Hallmann, C., Xie, S., Ruan, X., & Summons, R. E. (2015). Comparative microbial diversity and redox environments of black shale and stromatolite facies in the Mesoproterozoic Xiamaling formation. *Elsevier*, 151, 150–167.
- Luo, G., Yang, H., Algeo, T. J., Hallmann, C., & Xie, S. (2019). Lipid biomarkers for the reconstruction of deep-time environmental conditions. *Earth-Science Reviews*, 189, 99–124.
- Macko, S. A., Fogel, M. L., Hare, P. E., & Hoering, T. C. (1987). Isotopic fractionation of nitrogen and carbon in the synthesis of amino acids by microorganisms. *Chemical Geology: Isotope Geoscience Section*, 65, 79–92.
- Mahmoudi, N., Beaupré, S. R., Steen, A. D., & Pearson, A. (2017). Sequential bioavailability of sedimentary organic matter to heterotrophic bacteria. *Environmental Microbiology*, 19, 2629–2644.
- Mayali, X., Weber, P. K., Brodie, E. L., Mabery, S., Hoerich, P. D., & Pett-Ridge, J. (2012). High-throughput isotopic analysis of RNA microarrays to quantify microbial resource use. *ISME Journal*, 6, 1210–1221.
- Melzer, E., & Schmidt, H. L. (1987). Carbon isotope effects on the pyruvate-dehydrogenase reaction and their importance for relative C-13 depletion in lipids. *Journal of Biological Chemistry*, 262, 8159–8164.
- Mohr, W., Tang, T., Sattin, S. R., Bovee, R. J., & Pearson, A. (2014). Protein stable isotope fingerprinting: Multidimensional protein chromatography coupled to stable isotope-ratio mass spectrometry. *Analytical Chemistry*, 86, 8514–8520.
- Monson, K. D., & Hayes, J. M. (1982). Carbon isotopic fractionation in the biosynthesis of bacterial fatty-acids - ozonolysis of unsaturated fatty-acids as a means of determining the intramolecular distribution of carbon isotopes. *Geochimica Et Cosmochimica Acta*, 46, 139–149.
- Mouginot, C., Zimmerman, A. E., Bonachela, J. A., Fredricks, H., Allison, S. D., van Mooy, B. A. S., & Martiny, A. C. (2015). Resource allocation by the marine cyanobacterium *Synechococcus* WH8102 in response to different nutrient supply ratios. *Limnology and Oceanography*, 60, 1634–1641.
- Musilova, M., Tranter, M., Bennett, S. A., Wadham, J., & Anesio, A. M. (2015). Stable microbial community composition on the Greenland ice sheet. *Frontiers in Microbiology*, 6, 193.
- Nold, S. C., & Ward, D. M. (1996). Photosynthate partitioning and fermentation in hot spring microbial mat communities. *Applied and Environmental Microbiology*, 62, 4598–4607.
- Odden, W., Barth, T., & Talbot, M. (2002). Compound-specific carbon isotope analysis of natural and artificially generated hydrocarbons in source rocks and petroleum fluids from offshore mid-Norway. *Organic Geochemistry*, 33, 47–65.
- Osterhout, J., Schopf, J. W., Williford, K., McKeegan, K., Kudryavtsev, A. B., & Liu, M.-C. (2021). Carbon isotopes of Proterozoic filamentous microfossils: SIMS analyses of ancient cyanobacteria from two disparate shallow-marine cherts. *Geomicrobiology Journal*, 38, 719–731.
- Parenteau, M. N. (2007). *Microbial biosignatures in high-iron thermal springs*. Portland State University.
- Parenteau, M. N., & Cady, S. L. (2010). Microbial biosignatures in iron-impregnated phototrophic mats at chocolate pots Hot Springs, Yellowstone National Park, United States. *PALAIOS*, 25(2), 97–111.
- Parenteau, M. N., Jahnke, L. L., Farmer, J. D., & Cady, S. L. (2014). Production and early preservation of lipid biomarkers in iron hot springs. *Astrobiology*, 14, 502–521.

- Pawlowska, M. M., Butterfield, N. J., & Brocks, J. J. (2013). Lipid taphonomy in the Proterozoic and the effect of microbial mats on biomarker preservation. *Geology*, *41*, 103–106.
- Pearson, A., McNichol, A. P., Benitez-Nelson, B. C., Hayes, J. M., & Eglinton, T. I. (2001). Origins of lipid biomarkers in Santa Monica Basin surface sediment: A case study using compound-specific $\Delta^{14}\text{C}$ analysis. *Geochimica et Cosmochimica Acta*, *65*, 3123–3137.
- Pedentchouk, N., & Zhou, Y. (2020). Factors controlling carbon and hydrogen isotope fractionation during biosynthesis of lipids by phototrophic organisms. In *Hydrocarbons, oils and lipids: Diversity, origin, chemistry and fate* (pp. 99–122). Springer.
- Pereira, S., Zille, A., Micheletti, E., Moradas-Ferreira, P., De Philippis, R., & Tamagnini, P. (2009). Complexity of cyanobacterial exopolysaccharides: Composition, structures, inducing factors and putative genes involved in their biosynthesis and assembly. *FEMS Microbiology Reviews*, *33*(5), 917–941.
- Pedrosa-Pàmies, R., Conte, M. H., Weber, J. C., & Johnson, R. (2018). Carbon cycling in the Sargasso Sea water column: Insights from lipid biomarkers in suspended particles. *Elsevier*, *168*, 248–278.
- Penning, H., & Conrad, R. (2006). Carbon isotope effects associated with mixed-acid fermentation of saccharides by clostridium papyrosolvens. *Geochimica et Cosmochimica Acta*, *70*, 2283–2297.
- Perry, G. J., Volkman, J. K., & Johns, R. B. (1979). Fatty acids of bacterial origin in contemporary marine sediments. *Geochimica et Cosmochimica Acta*, *43*(11), 1715–1725.
- Pierson, B. K., & Castenholz, R. W. (1974). Studies of pigments and growth in *Chloroflexus aurantiacus*, a phototrophic filamentous bacterium. *Archives of Microbiology*, *100*, 283–305.
- Pierson, B. K., & Parenteau, M. N. (2000). Phototrophs in high iron microbial mats: Microstructure of mats in iron-depositing hot springs. *FEMS Microbiology Ecology*, *32*(3), 181–196.
- Pierson, B. K., Parenteau, M. N., & Griffin, D. B. M. (1999). Phototrophs in high-iron-concentration microbial mats: Physiological ecology of phototrophs in an iron-depositing hot spring. *Applied and Environmental Microbiology*, *65*, 5474–5483.
- Pinnegar, J. K., & Polunin, N. V. C. (2000). Contributions of stable-isotope data to elucidating food webs of Mediterranean rocky littoral fishes. *Oecologia*, *122*, 399–409.
- Radajewski, S., Ineson, P., Parekh, N. R., & Murrell, J. C. (2000). Stable-isotope probing as a tool in microbial ecology. *Nature*, *403*, 646–649.
- Reinhard, C. T., Planavsky, N. J., Gill, B. C., Ozaki, K., Robbins, L. J., Lyons, T. W., Fischer, W. W., Wang, C., Cole, D. B., & Konhauser, K. O. (2017). Evolution of the global phosphorus cycle. *Nature*, *541*, 386–389.
- Ruff-Roberts, A. L., Kuenen, J. G., & Ward, D. M. (1994). Distribution of cultivated and uncultivated cyanobacteria and chloroflexus-like bacteria in hot spring microbial mats. *Applied and Environmental Microbiology*, *60*(2), 697–704.
- Sakata, S., Hayes, J. M., McTaggart, A. R., Evans, R. A., Leckrone, K. J., & Togasaki, R. K. (1997). Carbon isotopic fractionation associated with lipid biosynthesis by a cyanobacterium: Relevance for interpretation of biomarker records. *Geochimica et Cosmochimica Acta*, *61*, 5379–5389.
- Schopf, J. W., Kudryavtsev, A. B., Czaja, A. D., & Tripathi, A. B. (2007). Evidence of Archean life: Stromatolites and microfossils. *Precambrian Research*, *158*, 141–155.
- Schuler, C. G., Havig, J. R., & Hamilton, T. L. (2017). Hot spring microbial community composition, morphology, and carbon fixation: Implications for interpreting the ancient rock record. *Frontiers in Earth Science*, *5*, 1–17.
- Sessions, A. L., Sylva, S. P., & Hayes, J. M. (2005). Moving-wire device for carbon isotopic analyses of nanogram quantities of nonvolatile organic carbon. *Analytical Chemistry*, *77*, 6519–6527.
- Shen, V. K., Siderius, D. W., Kregelberg, W. P., & Hatch, H. W. (Eds.). (2017). *NIST standard reference simulation website*. NIST Stand., National Institute of Standards and Technology.
- Shih, P. M., Ward, L. M., & Fischer, W. W. (2017). Evolution of the 3-hydroxypropionate bicycle and recent transfer of anoxygenic photosynthesis into the chloroflexi. *Proceedings of the National Academy of Sciences of the United States of America*, *114*, 10749–10754.
- Stal, L. J., & Moezelaar, R. (1997). Fermentation in cyanobacteria. *FEMS Microbiology Reviews*, *21*, 179–211.
- Steiner, M., & Reiter, J. (2001). Evidence of organic structures in Ediacara-type fossils and associated microbial mats. *Geology*, *29*, 1119–1122.
- Stuart, R. K., Mayali, X., Lee, J. Z., Craig, E. R., Hwang, M., Bebout, B. M., Weber, P. K., Pett-Ridge, J., & Thelen, M. P. (2016). Cyanobacterial reuse of extracellular organic carbon in microbial mats. *ISME Journal*, *10*, 1240–1251.
- Sturt, H. F., Summons, R. E., Smith, K., Elvert, M., & Hinrichs, K. U. (2004). Intact polar membrane lipids in prokaryotes and sediments deciphered by high-performance liquid chromatography/electrospray ionization multistage mass spectrometry - new biomarkers for biogeochemistry and microbial ecology. *Rapid Communications in Mass Spectrometry*, *18*, 617–628.
- Sun, Y., Chen, Z., Xu, S., & Cai, P. (2005). Stable carbon and hydrogen isotopic fractionation of individual n-alkanes accompanying biodegradation: Evidence from a group of progressively biodegraded oils. *Organic Geochemistry*, *36*(2), 225–238.
- Tang, Y., Huang, Y., Ellis, G. S., Wang, Y., Kralert, P. G., Gillaizeau, B., Ma, Q., & Hwang, R. (2005). A kinetic model for thermally induced hydrogen and carbon isotope fractionation of individual n-alkanes in crude oil. *Geochimica et Cosmochimica Acta*, *69*, 4505–4520.
- Tang, T., Mohr, W., Sattin, S. R., Rogers, D. R., Girguis, P. R., & Pearson, A. (2017). Geochemically distinct carbon isotope distributions in *Allochroamatium vinosum* DSM 180Tgrown photoautotrophically and photoheterotrophically. *Geobiology*, *15*, 324–339.
- Tarhan, L. G. (2018). The early Paleozoic development of bioturbation—Evolutionary and geobiological consequences. *Earth-Science Reviews*, *178*, 177–207.
- Teece, M. A., & Fogel, M. L. (2007). Stable carbon isotope biogeochemistry of monosaccharides in aquatic organisms and terrestrial plants. *Organic Geochemistry*, *38*, 458–473.
- Thomas, A. T., Ognibene, T., Daley, P., Turteltaub, K., Radousky, H., & Bench, G. (2011). Ultrahigh efficiency moving wire combustion interface for online coupling of high-performance liquid chromatography (HPLC). *Analytical Chemistry*, *83*, 9413–9417.
- Tian, C., Xia, Y., Song, C., Ma, S., Gao, W., & Xing, L. (2017). Changes in the carbon isotope composition of pristane and phytane with increasing maturity. *Petroleum Science and Technology*, *35*(12), 1270–1276.
- Tibocha-Bonilla, J. D., Kumar, M., Richelle, A., Godoy-Silva, R. D., Zengler, K., & Zuñiga, C. (2020). Dynamic resource allocation drives growth under nitrogen starvation in eukaryotes. *NPJ Systems Biology and Applications*, *6*, 1–9.
- van der Meer, M. T., Schouten, S., van Dongen, B. E., Rijpstra, W. I., Fuchs, G., Damste, J. S., de Leeuw, J. W., & Ward, D. M. (2001). Biosynthetic controls on the ^{13}C contents of organic components in the photoautotrophic bacterium *Chloroflexus aurantiacus*. *Journal of Biological Chemistry*, *276*, 10971–10976.
- van der Meer, M. T. J., Schouten, S., Jaap, S., Damsté, S., de Leeuw, J. W., & Ward, D. M. (2003). Compound-specific isotopic fractionation patterns suggest different carbon metabolisms among chloroflexus-like bacteria in hot-spring microbial mats compound-specific isotopic fractionation patterns suggest different carbon metabolisms among chloroflexus. *Applied & Environmental Microbiology*, *69*, 6000–6006.
- van der Meer, M. T. J., Schouten, S., Mary, M., Nübel, U., Wieland, A., Kühl, M., Leeuw, W., de Damsté, J. S. S., Ward, D. M., Bateson, M. M., Nu, U., Ku, M., de Leeuw, J. W., & Damste, J. S. S. (2005). Diel variations in carbon metabolism by green nonsulfur-like bacteria in alkaline siliceous hot spring microbial mats from Yellowstone National Park. *American Society for Microbiology*, *71*, 3978–3986.

- van der Meer, M. T. J., Schouten, S., Damsté, J. S. S., & Ward, D. M. (2007). Impact of carbon metabolism on ^{13}C signatures of cyanobacteria and green non-sulfur-like bacteria inhabiting a microbial mat from an alkaline siliceous hot spring in Yellowstone National Park (USA). *Environmental Microbiology*, 9, 482–491.
- van der Meer, M. T. J., Klatt, C. G., Wood, J., Bryant, D. A., Bateson, M. M., Lammerts, L., Schouten, S., Sinninghe Damsté, J. S., Madigan, M. T., & Ward, D. M. (2010). Cultivation and genomic, nutritional, and lipid biomarker characterization of Roseiflexus strains closely related to predominant in situ populations inhabiting yellowstone hot spring microbial mats. *Journal of Bacteriology*, 192, 3033–3042.
- van der Zanden, M. J., & Rasmussen, J. B. (2001). Variation in $\delta^{15}\text{N}$ and $\delta^{13}\text{C}$ trophic fractionation: Implications for aquatic food web studies. *Limnology and Oceanography*, 46, 2061–2066.
- van Dongen, B. E., Schouten, S., & Damsté, J. S. S. (2001). Gas chromatography/combustion/isotope-ratiomonitoring mass spectrometric analysis of methylboronic derivatives of monosaccharides: A new method for determining natural ^{13}C abundances of carbohydrates. *Rapid Communications in Mass Spectrometry*, 15(7), 496–500. Portico. <https://doi.org/10.1002/rcm.259>
- van Dongen, B. E., Schouten, S., & Sinninghe Damsté, J. S. (2002). Carbon isotope variability in monosaccharides and lipids of aquatic algae and terrestrial plants. *Marine Ecology Progress Series*, 232, 83–92.
- van Maldegem, L. M., Sansjofre, P., Weijers, J. W. H., Wolkenstein, K., Strother, P. K., Wörmer, L., Hefter, J., Nettersheim, B. J., Hoshino, Y., Schouten, S., Sinninghe Damsté, J. S., Nath, N., Griesinger, C., Kuznetsov, N. B., Elie, M., Elvert, M., Tegelaar, E., Gleixner, G., & Hallmann, C. (2019). Bisnorgammacerane traces predatory pressure and the persistent rise of algal ecosystems after snowball earth. *Nature Communications*, 10, 1–11.
- Větrovský, T., & Baldrian, P. (2013). The variability of the 16S rRNA gene in bacterial genomes and its consequences for bacterial community analyses. *PLoS ONE*, 8, e57923.
- Vinnichenko, G., Jarrett, A. J. M., van Maldegem, L. M., & Brocks, J. J. (2021). Substantial maturity influence on carbon and hydrogen isotopic composition of n-alkanes in sedimentary rocks. *Organic Geochemistry*, 152(104), 171.
- Werne, J. P., Baas, M., & Sinninghe Damsté, J. S. (2002). Molecular isotopic tracing of carbon flow and trophic relationships in a methane-supported benthic microbial community. *Limnology and Oceanography*, 47, 1694–1701.
- Whitman W. B., Parte A. C., Krieg N. R., Staley J. T., Brown D. R., Hedlund B. P., Paster B. J., Ward N. L., Ludwig W. (2010) *Bergey's manual of systematic bacteriology, volume four, the Bacteroidetes, Spirochaetes, Tenericutes (mollicutes), Acidobacteria, Fibrobacteres, Fusobacteria, Dictyoglomi, Gemmatimonadetes, Lentisphaerae, Verrucomicrobia, Chlamydiae, and Planctomycetes*. Springer.
- Wieland, A., Pape, T., Möbius, J., Klock, J. H., & Michaelis, W. (2008). Carbon pools and isotopic trends in a hypersaline cyanobacterial mat. *Geobiology*, 6, 171–186.
- Williford, K. H., Ushikubo, T., Schopf, J. W., Lepot, K., Kitajima, K., & Valley, J. W. (2013). Preservation and detection of microstructural and taxonomic correlations in the carbon isotopic compositions of individual Precambrian microfossils. *Geochimica et Cosmochimica Acta*, 104, 165–182.
- Zarzycki, J., & Fuchs, G. (2011). Coassimilation of organic substrates via the autotrophic 3-hydroxypropionate bi-cycle in *Chloroflexus aurantiacus*. *Applied and Environmental Microbiology*, 77(17), 6181–6188.

SUPPORTING INFORMATION

Additional supporting information can be found online in the Supporting Information section at the end of this article.

How to cite this article: Gonzalez-Nayeck, A. C., Mohr, W., Tang, T., Sattin, S., Parenteau, M. N., Jahnke, L. L., & Pearson, A. (2022). Absence of canonical trophic levels in a microbial mat. *Geobiology*, 20, 726–740. <https://doi.org/10.1111/gbi.12511>